Efficient and Realistic Brain Simulation

A Review and Design Guide for Memristor-Based Approaches

Landsmeer, Lennart Paul Liong; Siddiqi, Muhammad Ali; Abunahla, Heba; Negrello, Mario; Hamdioui, Said; Strydis, Christos

DOI
10.1002/admt.202401587

Publication date
2025

Document Version
Final published version

Published in
Advanced Materials Technologies

Citation (APA)
Landsmeer, L. P. L., Siddiqi, M. A., Abunahla, H., Negrello, M., Hamdioui, S., & Strydis, C. (2025). Efficient and Realistic Brain Simulation: A Review and Design Guide for Memristor-Based Approaches. *Advanced Materials Technologies*, *10*(17), Article e01587. https://doi.org/10.1002/admt.202401587

ADVANCED MATERIALS TECHNOLOGIES
www.advmattechnol.de

Efficient and Realistic Brain Simulation: A Review and Design Guide for Memristor-Based Approaches

Lennart Paul Liong Landsmeer, Muhammad Ali Siddiqi, Heba Abunahla, Mario Negrello, Said Hamdioui, and Christos Strydis**

Computational-neuroscience research is increasingly in need of larger, biophysically realistic brain models. These analog-in-nature models build upon the Hodgkin-Huxley (HH) formalism and are run on digital, high-performance computing systems making simulation very computationally expensive. In circuit form, these models are theoretically suitable for efficient analog implementation. However, the ion-channel components –predominantly, sodium and potassium– are nonlinear, time-varying resistors, lacking an efficient implementation. Chua et al. proved that these ion-channel models are in fact memristors –devices with a conductance as a function of applied-voltage history– claiming that "memristors are the right stuff for building brains". However, the kind of actual memristor implementation that is the right one for building brains is not defined. In this article, the device class and characteristics of such memristors are defined and existing memristive implementations of HH-like designs are then reviewed. Surprisingly, although often misclassified as such, no physical implementation currently exists that replicates the original HH equations faithfully or efficiently. Having put forward the desired memristor properties, a design guide for screening suitable memristor designs is then proposed. Screening the existing literature reveals that suitable devices likely already exist for potassium ion-channel emulation, while none exists for sodium; this calls for further investigation of higher-order, voltage-controlled and volatile memristors.

1. Introduction

Neuroscientific research requires *efficient* and accurate brain-simulation platforms.[23–26] Efficiency is measured in speed (actual versus biological), energy usage and hardware size, while accuracy depends on the level of modeling detailed captured in simulations. In terms of accuracy, brain models can be divided in simplified or biophysically realistic. Of the two classes, biophysically realistic models –with the most well-known being the Hodgkin-Huxley (HH) model[27]– differentiate themselves by explicitly modelling the ion channels (e.g., sodium and potassium) present in the neural membrane. They provide the most insight into the brain, allow for precise modelling of diverse neuron-types and transfer between therapeutic targets and clinical outcomes.[28,29] Given their recognised high accuracy,[23,25,30] there is a pressing need for efficient simulation platforms incorporating such biophysically realistic brain models.

The state of the art can be divided into digital and analog approaches. General-purpose, digital hardware has been the go-to method for brain simulation for the past 70 years. Initially simulated on CPUs,[1–4,31] the need for large-scale simulations of both simplified and biophysically realistic models, called for GPU (Graphics-Processing Unit),[4–6,32] later FPGA (Field-Programmable Gate Array)[7–11] and even AI-chip[33,34] based simulation platforms. As a specialized solution, digital neuromorphic chips have also emerged targeting simplified models.[17–19] However, since biophysical models essentially are electrical circuits, there are limits to the efficiency of their simulation in digital hardware.

To overcome this challenge, researchers have eventually turned to analog platforms. This led to specialized analog, neuromorphic chips targeting the simulation of simplified neural models.[13–16] Analog platforms for simulating biophysically realistic models have also been proposed but capturing the necessary ion-channel detail was so demanding that only a single neuron could be fit per chip.[20] Still, memristor technology has, more recently, led to single-device implementations of simplified neuron

L. P. L. Landsmeer, M. A. Siddiqi, H. Abunahla, S. Hamdioui, C. Strydis
Quantum and Computer Engineering Department
Delft University of Technology
Mekelweg 4, Delft 2628 CD, The Netherlands
E-mail: l.p.l.landsmeer@tudelft.nl

L. P. L. Landsmeer, M. A. Siddiqi, M. Negrello, C. Strydis
Department of Neuroscience
Erasmus Medical Center
Dr. Molewaterplein 40, Rotterdam 3015 GD, The Netherlands
E-mail: c.strydis@erasmusmc.nl

M. A. Siddiqi
Electrical Engineering Department
Lahore University of Management Sciences
Lahore 54792, Pakistan

The ORCID identification number(s) for the author(s) of this article can be found under https://doi.org/10.1002/admt.202401587

DOI: 10.1002/admt.202401587

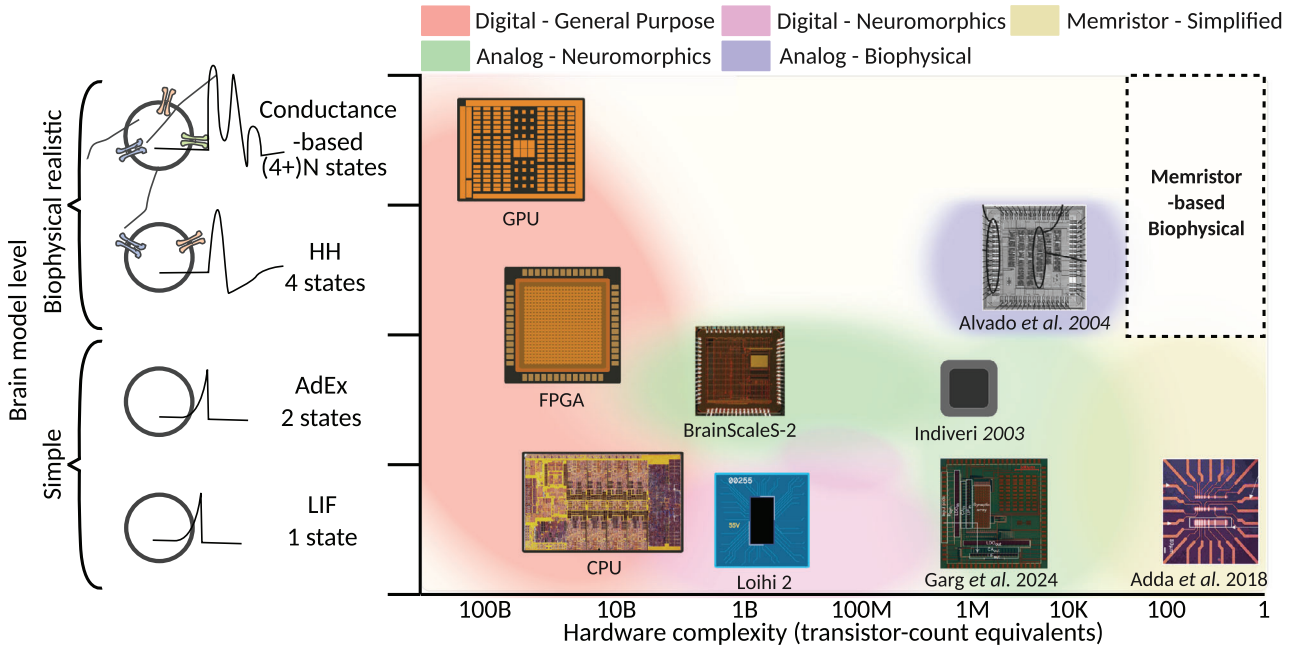

Figure 1. Lack of efficient platforms for biophysically realistic brain simulation: Landscape of available hardware for the simulation of brain-models at various levels of detail. X-axis: Hardware complexity measured in transistor-count or approximate transistor equivalents based on die-area and technology. Y-axis: Neuroscience models at various levels of biological detail, ranging from abstract simplified models to ion-channel based bottom up models. Digital - General Purpose including CPU,[1–4], GPU,[4–6] and FPGA[7–11] are available for all model levels. Seeking energy efficiency and miniaturisation, both *Analog Neuromorphics* (Garg et al., Copyright 2024, The Authors, and BrainScaleS-2, CC-BY 4.0[12])[13–16] and Digital Neuromorphics[17–19] platforms have been produced as a more specialized solution targeting simplified brain models. Few works exist that target analog implementations of biophysically realistic neurons, Analog Biophysical (Alvado et al., Copyright 2004, Elsevier).[20] As an emerging technology in neuromorphic computing, memristors-based solutions show high potential for simplified Memristor-based (Adda et al., Copyright 2018, Springer Nature)[21,22] circuits as well as Memristor-based Biophysical realistic brain models. This review explores how this last class of memristor-based HH-like platforms can be used for brain simulation. Figures reproduced with permission. Rights retained by the original copyright holders.

models, bringing their simulation efficiency close to that of the actual brain.[21,22]

In fact, memristor technology is especially promising for biophysically realistic brain simulation: The key insight is the fact that ion channels in such a model are, in essence, memristors.[35,36] Therefore, memristor-based hardware seems to hold promise as an analog substrate for facilitating accurate and efficient brain simulations. The problem is then to find the right memristor-device(s) for brain simulation. **Figure 1** summarizes the current state of the art and also highlights the gap in approaches.

This paper starts by putting together a detailed specification of the ideal memristor device(s) for realistic brain simulations and, thereafter, uses it to review and taxonomise existing approaches in literature. The work concludes by offering a practical guide to designers for identifying existing or new memristors that are suited for the task of simulating the HH ion channels. Concisely, the contributions of this work are:

- A specification of the ideal memristor device(s) for HH-based neural simulations.
- A review and taxonomy of related HH-like memristive implementations.
- A design guide for identifying existing memristor devices as candidates for HH ion-channel simulation and an initial exploration of published devices.
- Using this design guide, a potential class of candidates for potassium-channel-compatible memristors came to light.

The manuscript is organised as follows: In Section 2, we provide all necessary background information: the HH model, Chua's insight and generalisation over biophysically realistic brain models. Section 3 presents a detailed explanation and discussion of the essential memristor device switching behavior and characteristics necessary to efficiently implement ion channels in the HH model. We follow up with a literature review and a taxonomy of previous attempts at memristor-based neurons in Section 4. In Section 5, we provide a design guide for identifying suitable devices, showing that further research is still needed for the sodium-memristor replacement. We conclude the manuscript in Section 6.

2. Memristors for HH-Based Brain Simulation

To see why memristors are the ideal substrate for efficient and accurate brain simulation, we first need to go over the theory of brain modelling, focussing on the HH model. Then, we restate Chua et al.'s claim that ion-channels are memristors, and thus that memristors are the ideal substrate for brain-like systems. Finally, we generalise these arguments to biophysically realistic brain models.

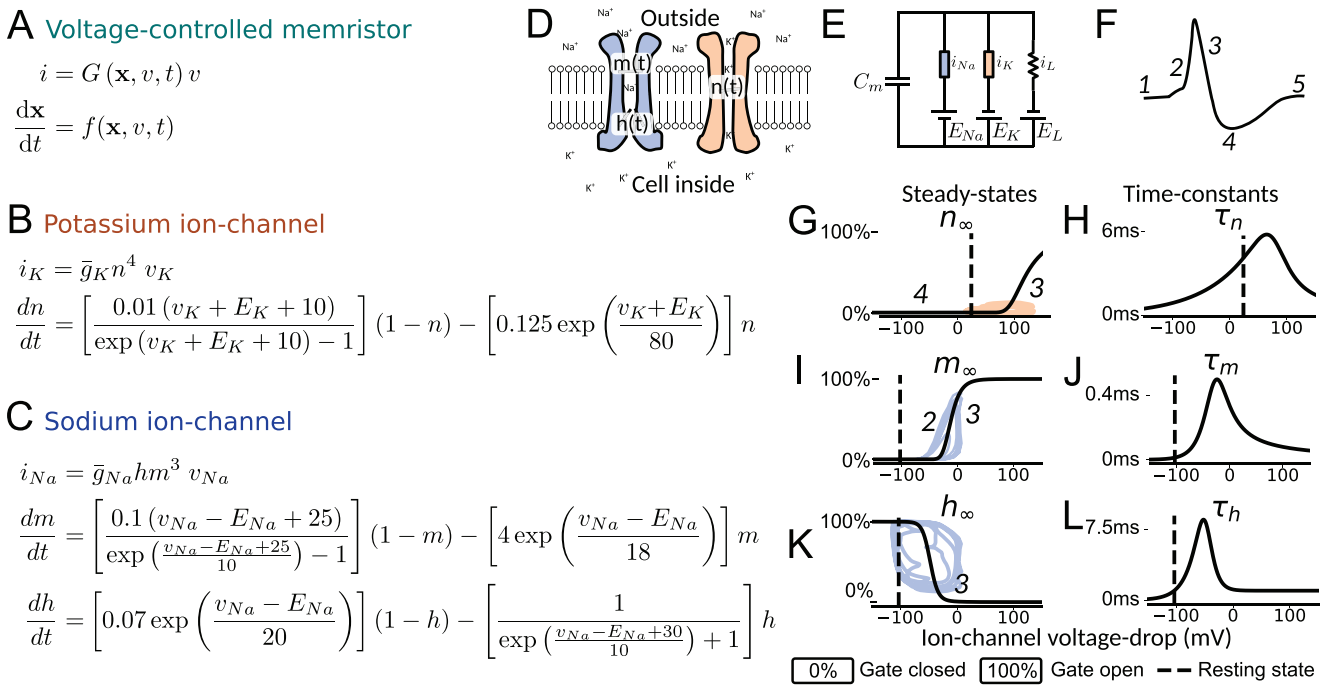

Figure 2. Memristors and the Hodgkin-Huxley model. Comparison between the memristive-system definition and the Hodgkin-Huxley ion-channel definitions. A) Equations shows the definition of a voltage-controlled memristive system – a memristor. Here, v is the input voltage, i is the output current, the vector x represents a set of state variables describing the memristor (e.g., the n, m and h gates in the case of Na and K channels), and $G(...)$ and $f(...)$ are continuous functions. B,C) Equations show the current-voltage relations of the potassium and sodium channels according to the HH model. E_{Na} and E_K are the reversal potentials of the sodium and potassium ions, the membrane potential difference at which no more net ion-flux occurs, represented as a battery/bias element. Activation functions are highlighted in square brackets. The resulting steady-state and switching-speed are visualized in (G–L). D) Schematic picture of the main components of the HH model: a membrane acting as a capacitor, two ion-channels functioning as nonlinear time-varying resistances and ions creating a potential difference across the membrane. E) Circuit representation of the HH model, which when simulated using the equations B and C, reproduces neural behavior. F) Resulting action-potential after a stimulus. G–L) Plots of the steady state and time-constants of the activation functions in B (G, H) and C (I, J, K, L). The zero-potential is taken as the corresponding reversal potential, meaning that the potential difference is measured across the ion channel instead of the usual cell-potential frame of reference. The striped, black, vertical lines correspond to the leakage-potential level, close to the resting potential. Colored traces show the recorder values over an actual noise-stimulus simulation run and thus the operation ranges. 1-5) *1*: resting state. *2*: action-potential initiation, depolarization and influx of sodium ions. *3*: repolarization and outflux of potassium ions. *4*: hyperpolarization. *5*: return to the resting state.

2.1. Hodgkin-Huxley Model and Extensions

A brain model builds on models of individual neurons, at the desired level of model accuracy to capture the essential components of biology under study. The two major classes are simplified and biophysically realistic models (including the HH model, see taxonomy in Ref. [30]). Simplified models concern the leaky-integrate-and-fire (LIF) model and its derivatives, while biophysically realistic modelling is epitomised in the HH model and its extensions (multiple channels and spatial neurons). The latter explain a neuron's behavior at the level of their constituent ion channels, and –if desired– take the full geometry of a spatial neuron into account. This allows them to capture a wide range of complex neural behavior not shown in simplified models, and also predict the outcomes to therapeutic targets via simulations of ion channel knockouts or in silico electrical stimulation. As such, biophysically realistic brain models have been one of the most popular models for both small and large-scale modelling of the brain due to trade-offs in computational complexity, explanatory power and interpretability against experimentally available data. For ease of understanding, the remainder of this section will focus on the prototypical biophysical realistic model –the HH model– while later generalizing to the broader model class (Section 2.3).

The original HH model is an electronic circuit, with common passive elements and two time-varying resistors modelling the ion channels. Here, we will briefly describe the different elements and how they correspond to the underlying biology (for more details, see. Ref. [27]) The neural-cell membrane, across which ion-concentration differences lead to the cell's membrane potential, is modelled as a capacitor. Passive ion transport across this membrane – the leakage channel – is modelled as a resistor connected to an external voltage reference. The sodium (Na^+) and potassium (K^+) channels are voltage-gated ion-channels, meaning their conductance changes according to the membrane potential. A large number of individual biological ion-channels are collapsed into a single HH-type ion-channel population, with internal variables describing statistical population averages. See **Figure 2**. A description of the potassium and sodium channels follows.

The potassium ion-channel models the voltage-gated flow of potassium ions across the cell membrane and is mostly

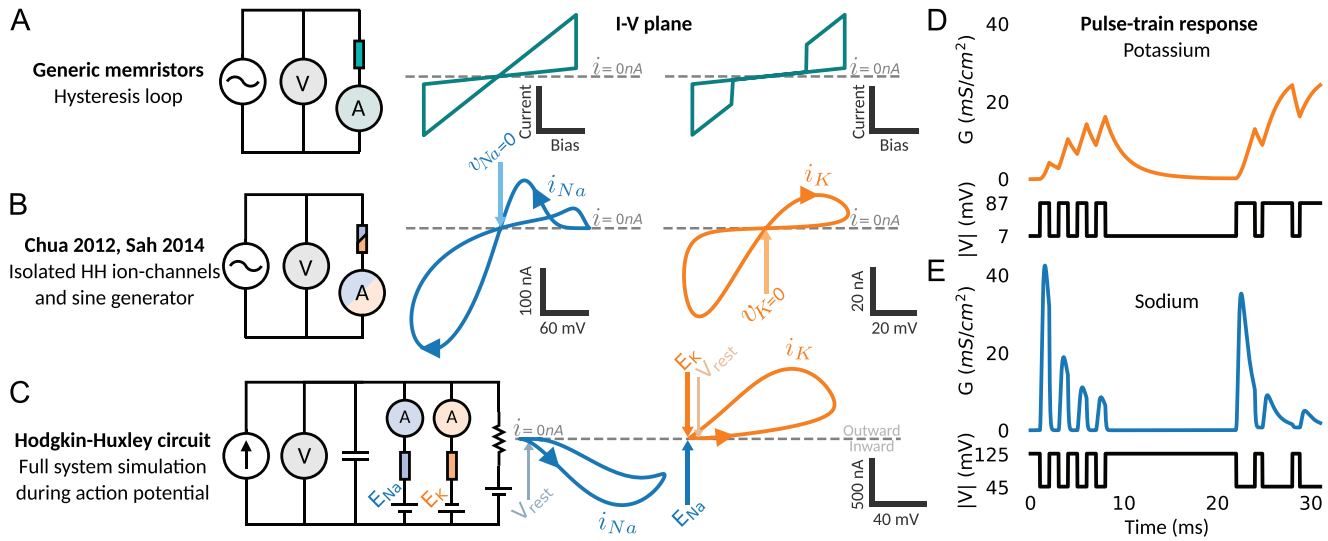

Figure 3. Ion Channels as Memristors: IV-plane (left) and conductance vs time (right). Left: IV-plane hysteresis loops of generic memristors (top), isolated ion channels (middle) and in full HH simulation (bottom). Right: Pulse-train response of the individual potassium (top) and sodium (bottom) ion channels, with pulse-voltages roughly corresponding to resting state and action-potential maximum. A) Prototypical ReRAM (left) and volatile (right) quasi-DC for sinusoidal input voltage. B) Initial experiments from Chua et al., showing that the individual ion-channels are memristors, by applying a sinusoidal input signal around zero. C) Full HH system with spike triggered due to input current. IV-plane is centred around the reversal potentials and thus shows the potential across the ion-channel. In grey, the resting potential is shown, which is the voltage across the device before an action potential. It can be seen that 1) the ion-channels do not cross the reversal potentials and thus bipolar or unipolar does not make a difference 2) the sodium memristor is biassed and closed in the resting state, while during an action potential, the channel starts temporarily conducting because of a reduced bias across the device. D) Pulse-train response of the potassium ion-channel to characterise dynamics in a way that can also be applied to candidate physical memristors. First a 500-Hz stimulation with 50% duty cycle is applied followed by a 250-Hz stimulation with 80% duty cycle. E) Inverted-pulse train response of the sodium ion-channel. Similar to the HH model, temporarily lowering the bias (an inverted pulse) across the device leads to quick opening and slow closing of the device. The same waveform is used as for the potassium channel but with different voltages corresponding more to the sodium ion-channel voltages. This behavior could serve as a benchmark for testing physical memristors in their suitability for HH simulation.

responsible for the refractory period of the neuron (Figure 2B,D–G). The ion channel has one gate (*n*), which can be open or closed. This gate is closed in the resting state (Figure 2-*1*) but at higher membrane potentials the gate slowly opens (Figure 2-*2,3*). The resulting outflux (a DC bias) of potassium ions leads to a drop in the membrane potential below the resting potential (Figure 2-*4*). The lower membrane potential then slowly closes the channel again, during which time it is not responsive to inputs (the refractory period). Now fully closed, the cell can return to its base state (Figure 2-*5*).

The sodium ion-channel models voltage-gated sodium ion-flow across the channel. In contrast to the potassium channel, it has two gates. At rest, one is open (*h*) and the other is closed (*m*). Once the cell nears its threshold voltage, the closed gate opens allowing sodium ions to flow into the cell leading to a rapid rise in cell voltage (Figure 2-2). The higher membrane potential causes the other gate to close, stopping the influx. At the same time, the potassium channel will bring the cell back to the refractory state, which is followed by the resting state (Figure 2-*3,4*). Finally, the sodium gates return to their original state (Figure 2-*5*).

The original HH model from 1952 has evolved beyond these two ion channels, and has become a framework for general, biophysically realistic neural models.[30] Notably, multiple channels corresponding to biological counterparts have been carefully developed, explaining not just the spiking behavior but many more aspects of cell behavior including subthreshold oscillations and spikelets, to name a few phenomena.[37,38] Spatial structures of cells can be replicated by discretizing the neuron shape into multiple smaller volumes following the HH dynamics, with resistors connecting these smaller volumes.[2,4] The general class of these models are now known as conductance-based or biologically realistic neurons.[30]

2.2. Ion Channels as Memristors

In a series of papers starting in 2012, Chua et al. outlined how the HH ion channels behave as voltage-controlled memristors.[35,36] They showed that the mathematical definitions of the two ion channels have the same form as the mathematical definition of a memristor. By simulating the individual ion channels with different inputs, pinched-hysteresis loops were shown to exist as well in the IV-plane, the hallmark of memristance (**Figure 3**A).[39] Therefore, they concluded that "memristors are the right stuff for building brain-like machines".

The key observation that the HH channels are indeed memristors is easily shown by factoring out the Na^+- and K^+-channels and comparing these to a memristor device. A memristor is a two-terminal device with a resistance that is a function of both the internal state variables and either voltage or current (respectively a voltage- or current controlled memristor). The internal state variables follow internal dynamics (a system of ordinary differential equations) based, again, on the internal state and the applied voltage or current (see Figure 2A). When we factor out

equations governing the Na^+- and K^+- channels (Figure 2B,C), we see indeed that they follow this general form: the channel current is derived by multiplying internal state variables with an overall maximum-conductance constant. The proof is trivially restated here: In Figure 2, Equations (B) and (C) are of the same mathematical form as Equation (A).

Consistently, also in simulation, do the two ion channels display behavioral characteristics of memristors: when an oscillatory voltage is applied (e.g., by substituting $v = A\sin(2\pi ft)$ with $A = 50$ mV and $f = 200$ Hz) separately to the two channels, the resulting steady-state shows a clear pinched-hysteresis loop in the I–V plane (Figure 3B). Going further, when applying more complex waveforms including biharmonic and rectangular waves, simulation reveals more complex phenomena including instantaneous switching modes, self-crossings away from the origin and loop reversals. Based on this observation, Sah et al.[36] concluded that memristors can approximate HH-modelled ion channels.

2.3. Generalisation over Biophysically Realistic Brain Models

Until now, the focus has been on the HH model, as it will be for the rest of this article. However, it is important to note that the previous arguments also hold for general biophysically realistic brain models, as will be demonstrated here. The prototypical equation solved by a brain-simulation software is known as the cable equation. It describes how ion channels, in the form of time-varying conductances, change the membrane potential on the surface of a neuron. The following guiding system of equations is the backbone of biophysically realistic neural models:[2,4,30]

$$C_m \dot{V} = \frac{\Delta_x V}{R_{\text{diff}}\left(\frac{\partial S}{\partial x}\right)} - \sum_k g_k(\mathbf{s}_k)\cdot(v - e_k) \tag{1}$$

$$\dot{\mathbf{s}_k} = \mathbf{f}_k(V, \mathbf{s}) \tag{2}$$

The partial differential equation (PDE) in Equation (1) denotes axial (x) voltage-diffusion ($\Delta_x V$) on the cell surface (S) and integration of ion-channel currents ($g_k(\mathbf{s}_k)(v - e_k)$) over the cell membrane (C_m), while Equation (2) shows the local-mechanism state ($\mathbf{s}_k$) dynamics. The channel-conductance ($g_k(\mathbf{s}_k)$) and state-dynamics ($f_k(V, \mathbf{s})$) functions are provided by the modeller and determine the specific ion channels. Again, this more general ion-channel definition still follows the definition of a memristor. The PDE in Equation (1) is solved in practice by discretisation, creating different compartments, each a small HH-like circuit, connected with resistors.[2,4,30] In theory, an entire spatial biophysically realistic neuron should be expressible using a memristor-based circuit, showing the great potential that memristor technologies have for brain simulation.

The calcium ion-channel, beyond the sodium and potassium ion-channel, has already been shown to be a memristor itself.[40] Another common extension to biophysical models, the inclusion of temperature-effects on channel dynamics, also leads to memristor behavior.[41]

In the following section, we will provide a detailed explanation of the memristive switching behavior and electrical characteristics needed to implement HH-model ion channels.

3. Device Specifications for HH-like Memristors

The ideal analog memristor-based implementation of the HH model or its derivatives is an exact copy of the HH formalizm in circuit form, where the nonlinear, varying resistors are replaced by physical memristors. The goal is to keep surrounding circuitry to a minimum so that the benefits of memristive technologies in *area use* and energy consumption are maximized. However, the fact that the HH ion channels are memristive systems does not mean that all memristors automatically qualify as valid ion-channel replacements or, even, that the ion channels have an efficient physical substitute.

The search for suitable analog memristor devices is a much harder challenge to tackle than implementing HH neurons in the digital domain on more traditional platforms, like CPUs, GPUs, or FPGAs. In that case, numerical approximations typically take place and, thus, we can build the system bottom-up using the HH equations as a guideline, at the same time providing a proof of the equivalence.

In contrast, physical memristors need to be produced top-down with behavior stemming from their materials and fabrication methods. While various physical memristor models exist at various scales, directly matching those to the HH equations at the level of device fabrication seems challenging at the moment. Instead, candidate-device selection has to be based on the careful exploration of desired electrical properties. Here, we give an overview of the most important device switching behavior and characteristics, which help us taxonomize different memristor device classes and narrow down to the ones of interest for HH ion-channel implementation.

The memristive-stack material combination and fabrication method both determine its characteristics, switching behavior and ultimately its device classification. Discovering a suitable HH-like memristor is necessarily a top-down approach since a general methodology that maps materials and fabrication methods to desired dynamics does not exist. For instance, in the HH formalizm, we model ion-channel dynamics as a Boltzmann distribution, which would be interesting to approximate by an analog memristor-switching mechanism. However, designing a switching mechanism on spec in an accurate and completely understood manner is still an open topic in the community. Here, we proceed to enumerate design specifications that can be measured, and thus validated, in fabricated memristor devices.

Electrical currents in biology are the result of ion transport as opposed to electron transport. The ion channels in the Hodgkin-Huxley model represent the population dynamics of different voltage-gated ion channels (for Na, K and all other ions). In biology, these voltage-gated ion-channels switch between an open and closed state, which is thermodynamically favored depending on the potential across the membrane. The Boltzmann distribution thus serves as a template for the ion-channel population dynamics as presented in the HH model, written as sigmoidal activation functions.

Control Mechanism: Memristive systems are usually classified as either current-controlled or voltage-controlled, meaning that

the resistance changes due to either current through or voltage across the device. In practice, a mixture of both is also possible (e.g., electrical-field-mediated ion migration at low bias and current-induced Joule heating leading to filament breakdown at high bias).

The voltage-gated ion channels modelled by the HH equations are clearly purely voltage-controlled. One could argue that in biology a single ion channel is also current-controlled as ions in the channel pores can prevent another ion from passing, but this has no observable population-level switching and is not taken into account in any HH-type model.

Depending on the mechanism, voltage-based switching can occur at distinct V_{set} and/or V_{reset} voltages. The potassium channel switches from OFF to ON after action-potential initiation, which is around 70–80 mV (Figure 2H). The sodium m-gate switches between −30 mV to 0 mV from OFF to ON (Figure 2J), and the sodium h-gate switches normally in reverse, i.e., from ON to OFF, at around −40 mV (Figure 2L).

Polarity: Memristors can be classified as either unipolar or bipolar (not to be confused with bistable). For a unipolar device, only the magnitude of the applied bias affects the conductance, while for a bipolar device, the bias directionality is also crucial to define the switching behavior. Unipolar means that there is no observable polarity in the device, while a bipolar device changes behavior based on its orientation. Both regimes can coexist in the same memristor, as the switching behaviors triggered by different voltage levels can result in different underlying switching mechanisms.[42]

The computational, HH ion-channel experiments performed by Chua et al.[35,36] clearly showed bipolar behavior, as is also evident from the equations (Figure 2A–C). In practice, we find that the ion channels never cross the origin in the *I*–*V* plane, making physical implementation independent of polarity; see Figure 3C. This might not hold for ion-channels different from sodium and potassium in more general biophysical models.

Volatility: Memristors can be classified as volatile or non-volatile. Most published devices are non-volatile, with resistive random-access memory (ReRAM) as the prototypical example.[42] This means that the device remembers its state when no bias is applied. A volatile device instead resets to its default state.

The HH ion-channel gate dynamics do not have multiple, coexisting, stable resistance states for any voltage value; this means that all gate equations are of the form $\dot{x} = (x^*(v) - x)/\tau(v)$, with thus only one stable point per voltage value. As such the ion channels should be classified as volatile. More generally, the HH ion-channels do not show hysteresis for any voltage value.

First-order, second-order or higher-order: Order relates to the amount of differential equations needed to describe the internal dynamics. This is most apparent in theoretical models, where the exact amount of differential equations is spelled out. Published memristor devices are reported up to 4th order.[43]

The order of HH channels related to their gate count (each having one state variable), and as such, the potassium channel is a 1st-order (one-gate) memristor and the sodium channel is a 2nd-order (two-gate) memristor.

Switching speed: Different memristor devices can take different time spans to switch between resistance states given the applied bias or current.

In the HH model, switching-time constants depend on the applied bias. The potassium-channel switching speed is around 4 ms at the resting state, slowest at the switching point at 6 ms and reaches 2 ms at the peak of the action potential (Figure 2H). The sodium channel has two gates, each with its own switching speed. The fast *m* gate behaves like the potassium-channel gate but with speeds ranging between 0.01 and 0.5 ms (Figure 2J). The slower *h* gate normally takes around 1 ms to switch but slows down to 6 ms at the switching point (Figure 2L). Exact matching of the switching speed curves seems like a far stretch with the level of control over device characteristics using current fabrication methods, and the designer should only try to keep the most essential parts of the curves as determined by appropriate simulation methods. Among others, the works in Section 4.1.1 show that rough approximations to the activation functions still result in the desired behavior over operation ranges.

Dynamics and Negative Differential Resistance: The potassium ion channel follows common volatile memristor dynamics reasonably well: application of a bias switches the device from a High-Resistance State (HRS) to a Low-Resistance State (LRS), whereas removing the bias resets the device to the HRS again (Figure 3D). The sodium ion channel, due to its second-order nature, has an activating–deactivating dynamics (Figure 3E). At the neural resting state, a bias is applied due to the sodium reversal-potential element, and the device is in the HRS. Lowering, or further removal of the bias leads to a quick switch (activating) to the LRS, followed by a slower switching to the HRS while keeping the bias removed. Re-application of the bias at any point moves the device to the HRS.

The fast activation of the sodium channel in response to lower bias, is due to the negative differential resistance (NDR) of the *m* gate (Figure 3I). NDR is visible as a negative differential relation in the IV-plane. Moreover, this can exhibit as either a *S-type* (current-controlled) NDR or *N-type* (voltage-controlled) NDR. For the fast activating gate of the sodium channel, from both the channel being voltage-controlled and the shape in the IV-plane, is of N-type NDR.

ON/OFF Ratio and Endurance: HH model shows ratios between HRS and LRS that are maximally ≈10 in practice, and, therefore, a high ratio is not a significant requirement. On the other hand, high endurance, which represents the expected switching cycles before device break-down, is desired for the HH model. Some neurons reach spike frequencies up to a few hundred Hz of continuous spiking, corresponding to multiple billion switch cycles over a year. This is a large upper bound, but still, a correct memristor needs to be able to handle many device cycles.

4. Related Work

In the previous section, we established a desired device class of a voltage-controlled, volatile, physical memristor. In this section, we provide an extensive review of related works, that is, memristor implementations of neurons. We generally identify and focus on three approaches to the design problem: theoretical templates, emulated memristors and physical memristors. A summary of the latter two using the above taxonomy is presented in **Table 1**.

Table 1. Summary of device taxonomy and memristive HH implementations. * Bipolar in theory, but unipolar would work as well in operational ranges (Figure 3C). † Mott-memristor operated in parallel with local capacitor to form ion-channel, making the channel second-order channel – could also be interpreted as a first order memristor. ‡ *Na* channel was implemented as a 555-Timer and not as a memristor.

	Material	Control	Polarity	Memory	Order	NDR type
K/Na[27]	Protein	Voltage	Bipolar*	Volatile	1/2	None/N
Hu 2019[47]	Emulation	Voltage	Bipolar	Volatile	1/2	None/N
Xu 2023[51,52]	Emulation	Voltage	Bipolar	Volatile	1/2	None/N
Li 2024[53]	Emulation	Voltage	Bipolar	Volatile	1/2	None/N
Picket 2013[44]	Pt/NbO_2/Pt	Current	Unipolar	Volatile	2/2 †	S/S
Feali 2017[54]	Pt/NbO_2/Pt	Current	Unipolar	Volatile	2/2 †	S/S
Yi 2018[45]	Pt/VO_2/Pt	Current	Unipolar	Volatile	2/2 †	S/S
Huang 2019[55]	W/WO_3/PEDOT:PSS/Pt	‡Voltage	‡Bipolar	‡Volatile	‡1/‡	None/‡
Yang 2024[46]	Ti/Pt/HfO_2/NbOx/Ti/Pt	Current	Bipolar	Volatile	2/2	S/S †

4.1. Memristor Models for Ion Channels

Not all related works targeting memristors for HH ion-channel simulation led to implementable designs, yet they still provide theoretical insights into the matter. An early attempt at designing a memristor exactly following the HH ion-channel dynamics from nonlinear circuit theory dates back to 2013.[48,49] The authors draw up a hypothetical, passive, two-port memristor, consisting of five nonlinear voltage-controlled resistors and one linear dynamic one-port ($i(v) = Y(d/dt)v$). This model is then parameterised to match the HH equations. While no physical correspondence is given to these nonlinear resistors, it does hint that a memristive implementation of sodium and potassium ion-channels should be possible in reality. A similar approach is taken by Liu et al.,[50] who make a memristor model from two diodes, a capacitor and an inductor. This memristor model is then used to build a memristive oscillator. A full neuron is simulated using the memristive oscillation. While behavior is far from biological, properties like bursting oscillations are observed. These theoretical works did not attempt to synthesize such memristive devices in reality and can thus not be used for HH simulation, yet they show that the memristive properties sought after are of bounded complexity.

4.1.1. Discrete-Component Memristor Emulation

Memristive properties do not have to derive from a single physical device; a memristor can also be emulated using discrete components. By replacing the sigmoidal Boltzmann activation functions of the ion-channels (see Figure 2) by much simpler, scaled exponents, a Simplified Memristive Hodgkin-Huxley neuron was designed using memristors made from analog components including multipliers and opamps.[47] Using SPICE-based simulation, the authors show that within operational ranges, the distortion is limited and spiking is retained.

The works of Xu et al.[51,52] go even further and implement the activation functions of the ion-channels using analog tanh function modules, and provide a fully analog implementation using discrete components on a breadboard. Their analysis indeed shows a multitude of biological realistic firing behaviors. A memristor-modelling approach based on transistors was also similarly used to implement HH-like behavior, with the further addition of a Calcium-T ion channel to the standard HH model.[53]

These techniques show that by designing the systems bottom-up, the resulting system could be compared directly to the targeted system at the mathematical level, guiding the design effort and providing limits on modelling-error. Concluding, we find highly accurate neuron implementations using discrete-component-based neurons. However, by using different components for constructing a memristors instead of using a physical single memristor device, promised efficiency gains are not captialised on.

4.1.2. Physical Memristors

Physical memristor-based designs are summarized in **Figure 4**. When targeting biorealistic neuron-like behavior, research has mostly focused on Mott-insulator memristors (the Mott-memristor approach). The Mott memristor is a volatile, first-order, S-type NDR, threshold-switching memristor, capable of a variety of behaviors[56,57]. Among others, when coupled to a capacitor, it creates an Pearson-Anson oscillator [58] This is then used as a building block for creating ion-channel-like behavior. Pickett et al.[44] pioneered the Mott-memristor approach to biorealistic neuron implementations. Inspired by the HH formalism, they set out to build a neuristor, an axon-like signal transmission line.[59] Using two NbO_2 memristors, oscillators corresponding to sodium and potassium channels are built to create an all-or-nothing-firing cell.[60] By connecting multiple such devices with resistors, a neuristor transmission line is formed, which shows axon-like spike transport. Others extended this work by adding noise to a simulation of the used memristors,[56] building what the authors call a 'Realistic Hodgkin–Huxley Axons'.[54] Importantly, these works show one of the key principles of conductance-based neural modelling: by combining multiple HH models, spatially elongated structures can be built that mimic biological signal propagation (Section 2.3). Attempting to overcome the LIF limitation[60] of the NbO_2 memristors, Yi et al.[45] set out to add more biological plausibility using VO_2-based memristors. The design follows more closely the original HH circuit design, with an extra capacitor and a resistor between the ion-channels. As a result, a large range of biologically plausible spiking behavior is observed, including bursting and frequency adaptation. Rehashing the potential of efficient memristor-based brain-like systems, the authors project competitive or better energy-usage per spike than the brain. Extending on this thread of work, in 'Fully Integrated Memristive Hodgkin-Huxley Neurons with Homeostatic Plasticity', Yang et al.[46] extend the Mott-memristor approach with two ReRAM memristors to make the neuron display homeostatic plasticity. By removing the capacitors from earlier designs, letting the parasitic capacitances of each device take on the role of a 'local' membrane, their design only uses four devices per neuron. S-type NDR is not only limited to Mott-insulator memristors. For example, perovskite memristors also show oscillations in a Pearson-Anson configuration, allowing for single memristor neuristor implementation.[61] Finally, Ascoli et al.[62] present

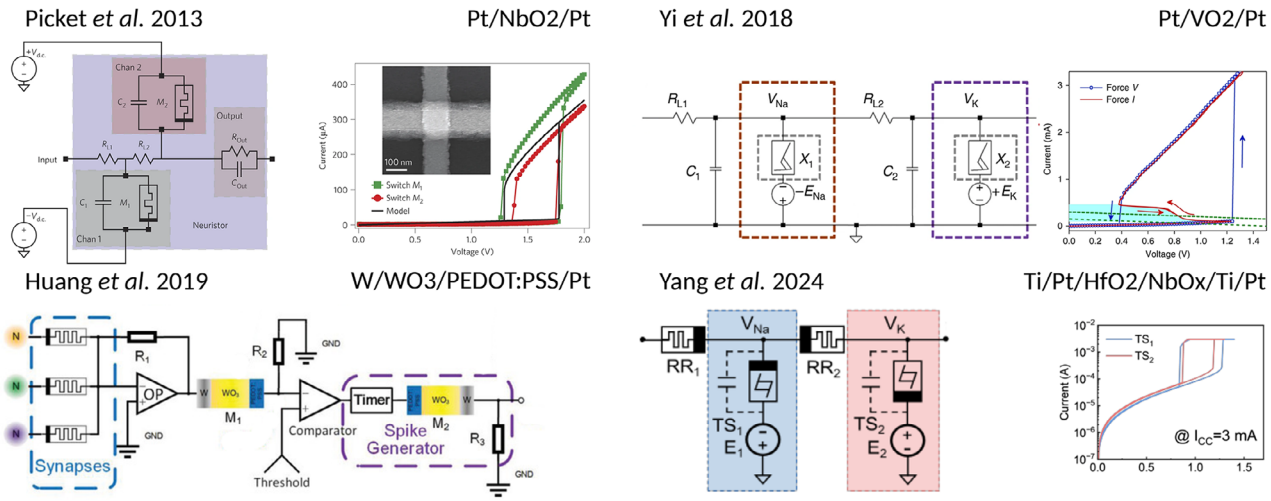

Figure 4. Physical-Memristor Designs for Biorealistic Neurons. Picket et al.[44] pioneered using Mott-memristors for HH-like spiking behavior. Copyright 2012, Spinger Nature. Yi et al.[45] followed up with more biorealistic behavior by using VO_2-based devices. CC-BY 4.0. Yang et al.[46] extended this line of work by placing two ReRAM memristors between the Mott-memristors for added homeostatic plasticity. Copyright 2024, IEEE. Huang et al.[47] take another approach based on WO_3/PEDOT:PSS in combination with a 555-based timer circuit Copyright 2018, WILEY. Common to Mott-memristor designs is a local capacitor –either parasitic or discrete– in parallel to each threshold-switching memristors, and the two memristors connected via a resistor or ReRAM element. This is in contrast to the HH-circuit representation where a single grounded capacitor is connected to both memristors, without a resistive element between the ion channels (Figure 2). Reproduced with permission. Rights retained by the original copyright holders.

an analysis or the 'First and Simplest Ever Reported Hodgkin–Huxley Neuristor', showing that also a design utilizing a single NbOx threshold-switching memristor, could recreate the behavior of the original Picket et al.

An exception to the Pearson-Anson oscillator-based approaches to HH is what the authors call a quasi-Hodgkin-Huxley neuron: a 555-timer circuit with a W/WO_3/PEDOT:PSS memristor that shows timer-generated spikes followed by memristor-mediated depolarization.[55] The depolarization is the result of the voltage-controlled, volatile behavior of the memristor. This is, thus, a quasi-ideal implementation.

4.2. Mott-Memristor Approach Criticism

In published physical memristors, we find higly efficient designs with energy usage competitive to the biological brain[45] and very low complexity.[46] We find the Mott-memristor approach[44–46,54,62] emerging as a platform for building HH-like neurons. While a promising path to the ideal HH implementation, there are however a few arguments against their use as a substrate for efficient and accurate brain simulation – a different goal from building efficient brain-like computing systems. These are based on the Mott-memristor characteristics, circuit form, and displayed 'biorealistic' behavior.

First, Mott-memristors switch based on current flowing through the memristor (Joule heating resulting in a Mott-transition). This is opposite to voltage-based switching seen in biology. Neurons built using Mott-memristors can not be HH neurons,[63] and this is also obvious given the electrical characterization given in Section 5. Furthermore, the second-order dynamics displayed by the Potassium channel oscillator do not match the expected first-order dynamics and multiple unbiological artefacts are present in generated spikes. Second, at the circuit level there are large differences: the HH model only contains a single capacitor, and the capacitor and ion-channels all terminate at the same circuit node, without resistors in between. There is no 'local membrane potential' for each channel type. Clearly the two ion-channels in the HH model are different (Section 3), while the memristors used in Mott-memristor designs are of similar build. Lastly, some works show a wide range of spiking behaviors and adaptation.[45,46] These more biorealistic behaviors could potentially lead to more compact computing applications, but are not part of the HH model itself. Within the biophysically realistic brain modelling framework, these would instead be characterized as extra ion-channels or the scaling of ion-channel conductances – not the result from the sodium and potassium channels or intermediate ReRAM memristors.

As such, while the voltage trace of a Mott-memristor based design might resemble that of the HH model, it is not an HH model in itself and thus is not an accurately model a neuron. With that, it loses some of its most important properties of biophysically realistic brain models: extensibility, and biological realism. We can thus conclude that the ideal efficient and accurate memristor for brain simulation has not yet been found.

5. Design Guide and Initial Exploration of Existing Devices

The detailed review conducted in Section 4 reveals that, since Chua et al.'s realisation that the ion channels in the HH model are memristors, multiple works have emerged targeting these topics. Two major approaches were found to implement HH-like systems using memristor technology: 1) works building the system bottom-up using emulated memristors, and 2) works using physical memristors in place of the ion channels, yet these memristors could never replicate the full HH behavior from a

device-class perspective since they cannot replicate the HH ion-channel characteristics, as laid out in Section 3.

Despite the fact that multiple review papers exist that misclassify various existing memristor designs as HH implementations,[64–66] as of yet we have found no design that correctly models HH ion channels. The ideal memristor-based HH implementation directly replaces the ion channels with physical memristors. Given the large body of published memristor devices and (un)explored design space, it still seems unclear which memristor to use for brain simulation, if any exists at all. A comprehensive characterization of memristors suitable for modelling HH ion channels seems to be lacking in the physical-memristor sub-literature. In this section, we will describe how the device characteristics from Section 3, in combination with a test bench, could be used for memristor-device design, selection, and validation.

5.1. A Top-down Approach to Memristor Selection for Ion Channels

As stated in Section 3, the voltage-gated ion channels in the HH formalism are voltage-controlled volatile memristors, with the order equal to their dynamic gate count. Other device specifications like switching thresholds and time-constants do not need to be translated directly into every aspect of a physical device. For example, one could decide to rescale time or voltage ranges, resulting in effectively the same behavior. Other characteristics like the exact activation-function shape probably also leave some room for error, as was seen in Section 4.1. Most importantly, a device needs to be found that falls within the desired memristor class, after which it can be tuned to specification.

5.1.1. K^+-Channel Memristor Candidates

Having provided detailed device specifications for HH-ion-channel replacement, here, we will go over existing memristor designs through the lens of this specification list. The potassium channel is a first-order, volatile, voltage-controlled memristor. The LRS is observed after applying a bias. Several applications have similar requirements, including synaptic plasticity, reservoir computing and some simplified neural-models.[67] For these, memristors are readily available. For example, certain WOx[68] or NbOx [69] memristors show a volatile, voltage-controlled switching mechanism via oxygen-vacancy drift-diffusion, resulting in potentiation under bias and decay under removal of bias. This is very similar to the required pulse-train response from Figure 3D for potassium ion-channel emulation. While the authors of these memristor devices show applicability in reservoir computing or synaptic plasticity, they did not validate the usefulness of these devices for potassium ion-channel emulation; for example by recording the current-response after applying a similar voltage trace obtained from a HH simulation or performing a HH simulating with the potassium ion-channel replaced by a model of such memristors. As such, it seems reasonable that the memristor technology is ready for this part of the HH model, however, potential candidates are not screened for eligibility; no HH-based analysis of the suitability of first-order, voltage-controlled, volatile memristors was found in literature for the potassium channel.

Table 2. Search for sodium ion-channel candidates: second-order voltage-controlled volatile memristors. While all design match w.r.t. these design specifications, the dynamics are different, meaning these are not fit as sodium replacements. * means the authors did not determine the identity of the state variable.

Material	States	Model	Refs.
Oxide-based			
Pt/WO_3/W	Schottky, oxygen	✗	[72]
Pt/STO/Nb-STO	Schottky, oxygen	✓	[73]
Pd/WOx/W	CF area, Vo mobility	✓	[74]
alpha-IGZO	w, *	—	[75]
Pd/TaOx/Pd	w, *	—	[76]
Ferroelectric			
LSMO/BTO/LSMO	Polarization and interface charge trapping	✗	[77]
W/aSi:H/HZO/TiN		✗	[78]
Si/HZO/TiN		✓	[79]

5.1.2. Na^+-Channel Memristor Candidates

Similarly to the potassium-channel case, existing memristor designs might already satisfy the requirements for the sodium channel, which is a second-order, volatile, voltage-controlled memristor. Furthermore, it has an activating-deactivating mechanism: at rest, it is operated in the HRS due to an applied bias. When the bias lowers, the sodium channel rapidly starts to conduct, after which it slowly closes again (Figure 3E). Crucially, the direct memristor replacement for the sodium channel is a second-order memristor, which severely reduces the amount of existing designs. In comparison to ReRAM-based devices, higher-order memristors have not received similar research attention.[70] Two major memristor switching mechanisms that depend on voltage instead of current are the valency-change mechanism (VCM) and the ferroelectric-effect[42,71]. Here, we review published VCM- and Ferroelectric-effect-based, second-order memristors; see **Table 2** for a summary. For a general review of higher-order dynamics, we point the reader to Ref. [43, 70].

For oxygen-ion/vacancy VCM-based memristors, several works are known.[72–76] Earlier designs[75,76] attributed second-order effects to an unknown extra state variable called *T*. Later design based on a Pd/WOx/W-memristor[74] claimed the state variables were the conductive-filament (CF) area and oxygen-vacancy mobility, of which they provided a mathematical model. In other models,[72,73] non-CF VCM-switching is attributed to the oxygen-ion distribution in the switching layer and modulation of the Schottky barrier at the interface. For the first time, direct observation of such effects was reported in a Pt/WO_3/W-memristor,[72] validating their model. In the latter three cases, all second-order switching is thought to be fully voltage-controlled. In the ferroelectric domain, second-order effects are attributed to polarization and trapping of oxygen ions at the interface. The second-order effects results from redox reactions or other mechanisms at the surface, due to excess oxygen-ion/vacancy charge-buildup after electrical-field induced migration. Again, second-order effects are thought to be voltage-controlled.

For both types of memristors, we find nearly independent effects, acting as superimposed volatile memristors. One exception is the Pd/WOx/W-memristor of Duet al.,[74] where the oxygen-migration and conductive-filament equations have a cross-dependency. Thus, physical voltage-controlled second-order volatile memristors do exist. While these are a step in the right direction, the desired activation-deactivation dynamics of the sodium ion-channel are still absent as the second-order mechanisms operate in the same 'activating' way. Research on how to introduce a fast N-type NDR, deactivation mechanism, on second-order voltage-controlled volatile memristors is thus needed.

5.1.3. Overcoming Challenges in Fabrication

Memristor device fabrication encounters fundamental challenges,[80] including variability due to material properties and process control, latency due to wire resistances and non-linearities, and density constraints that impact scalability and cost. These are well-known hurdles in neuromorphic hardware, but when designing memristors to mimic biological ion channels, additional complexities arise. For instance, biological ion-channels operate on millisecond timescales,[27] whereas most memristors function at orders of magnitude faster.[42] Engineering devices with realistic ion transport kinetics that match neural processing speeds is essential for accurate biomimicry of neural systems. Furthermore, unlike biological ion channels that regenerate naturally, memristive devices must maintain stable ionic transport over repeated switching cycles. Avoiding ion-trapping, material degradation, and unwanted diffusion is critical.

Despite these challenges, the highlighted devices under Section 5.1.1, show fabrication is possible for promising candidate devices, probing further validation. For future large-scale fabrication and integration, it is essential to ensure high endurance and yield.[81,82] Moreover, while device-to-device and cycle-to-cycle variations are often cited as major challenges for the adoption of memristors in end-user applications,[81,83] these issues may be less critical in the context of biologically realistic system simulations. Such systems naturally operate in noisy environments,[84] and the inherent noise-resilience of brain networks may accommodate this variability.[85] It appears that the ability to build robust, reproducible, and scalable ion-channel-mimicking memristors is within reach, paving the way for more biologically realistic neuromorphic computing.

6. Conclusion

In this work, the claim was reasserted that memristor devices hold enormous potential in becoming essential building blocks for efficient, biophysically realistic brain simulation.[35] A large gap in previous works was identified: although many past works have claimed to have developed HH-suitable memristor devices, none of them measure up to the specifications of an HH-based neuron model, as used in practice. To illustrate this point, an exhaustive HH-device specification was put together that helps identify the fabrication properties essential for correctly behaving HH memristors, followed by a detailed survey and taxonomy of related works. By analysing previous works against material and fabrication properties of memristors, the survey concluded that there are no existing memristor proposals for constructing analog, memristor-based HH neurons.

Therefore, the next step was to draw design guidelines for the 'ideal memristors' needed to construct HH-style neurons realizing that, in contrast to more traditional technologies, physical-memristor replacements for the HH ion channels require a top-down design approach. Search criteria including a testbench were fully specified so that materials researchers can check the suitability of their device(s) for HH simulation. Interestingly, on following the proposed search strategy, it was found that potassium-channel-compatible memristors likely already exist but sodium-channel memristors still require materials research into higher-order memristor mechanisms.

Acknowledgements

This work was supported by the European-Union Horizon Europe R&I program through projects SEPTON (No. 101094901), SECURED (No. 101095717) and through the NWO - Gravitation Programme DBI2 (No. 024.005.022), and the Erasmus MC Convergence Health and Technology Integrative Neuromedicine Flagship Program.

Conflict of Interest

The authors declare no conflict of interest.

Author Contributions

L.P.L.L. led the investigation, was involved in conceptualization, took the lead in writing the original draft, and participated in review and editing. M.A.S. and H.A. were involved in conceptualization, supported the investigation and original draft, and participated in review and editing. M.N. and S.H. were involved in conceptualization and participated in review and editing. C.S. was involved in conceptualization, supported the original draft, and participated in review and editing.

Keywords

brain simulation, dynamical system, hodgkin-huxley, memristor

Received: September 30, 2024
Revised: April 28, 2025
Published online:

[1] M.-O. Gewaltig, M. Diesmann, *Scholarpedia* **2007**, *2*, 1430.
[2] N. T. Carnevale, M. L. Hines, *The NEURON book*, Cambridge University Press, Cambridge **2006**.
[3] S. Panagiotou, H. Sidiropoulos, D. Soudris, M. Negrello, C. Strydis, *Front Neuroinform* **2022**, *16*, 724336.
[4] N. Abi Akar, B. Cumming, V. Karakasis, A. Küsters, W. Klijn, A. Peyser, S. Yates, in *2019 27th euromicro international conference on parallel, distributed and network-based processing (PDP)*, IEEE, Piscataway, NJ **2019**, pp. 274–282.
[5] B. Golosio, G. Tiddia, C. De Luca, E. Pastorelli, F. Simula, P. S. Paolucci, *Front Comput Neurosci* **2021**, *15*, 627620.

[6] P. Kumbhar, M. Hines, J. Fouriaux, A. Ovcharenko, J. King, F. Delalondre, F. Schürmann, *Front Neuroinform* **2019**, *13*, 63.
[7] A. Cassidy, S. Denham, P. Kanold, A. Andreou, in *2007 IEEE Biomedical Circuits and Systems Conference*, IEEE, Piscataway, NJ **2007**, pp. 75–78.
[8] A. Carpegna, A. Savino, S. Di Carlo, in *2022 IEEE Computer Society Annual Symposium on VLSI (ISVLSI)*, IEEE, Piscataway, NJ **2022**, pp. 14–19.
[9] Y. Liu, Y. Chen, W. Ye, Y. Gui, *IEEE Transactions on Circuits and Systems I: Regular Papers* **2022**, *69*, 2553.
[10] B. Ahn, in *International Conference on Neuromorphic Systems 2020*, ACM, Oak Ridge, TN, **2020**, pp. 1–8, https://doi.org/10.1145/3407197.3407223.
[11] R. Miedema, G. Smaragdos, M. Negrello, Z. Al-Ars, M. Möller, C. Strydis, *IEEE Access* **2020**, *8*, 121905.
[12] S. Billaudelle, B. Cramer, M. A. Petrovici, K. Schreiber, D. Kappel, J. Schemmel, K. Meier, *Neural Netw.* **2021**, *133*, 11.
[13] G. Indiveri, in *Proceedings of the 2003 International Symposium on Circuits and Systems, 2003. ISCAS'03.*, vol. *4*, IEEE, Piscataway, NJ **2003**, pp. IV–IV.
[14] Z. Yang, Y. Huang, J. Zhu, T. T. Ye, in *Proceedings of the 2020 on Great Lakes Symposium on VLSI*, ACM, New Orleans, LA, 2020, pp. 469–474.
[15] N. Garg, D. Florini, P. Dufour, E. Muhr, M. Faye, M. Bocquet, D. Querlioz, Y. Beilliard, D. Drouin, F. Alibart, J.-M. Portal, *arXiv preprint arXiv:2406.19667* **2024**.
[16] C. Pehle, S. Billaudelle, B. Cramer, J. Kaiser, K. Schreiber, Y. Stradmann, J. Weis, A. Leibfried, E. Müller, J. Schemmel, *Front Neurosci* **2022**, *16*, 795876.
[17] F. Akopyan, J. Sawada, A. Cassidy, R. Alvarez-Icaza, J. Arthur, P. Merolla, N. Imam, Y. Nakamura, P. Datta, G.-J. Nam, B. Taba, M. Beakes, B. Brezzo, J. B. Kuang, R. Manohar, W. P. Risk, B. Jackson, D. S. Modha, *IEEE transactions on computer-aided design of integrated circuits and systems* **2015**, *34*, 1537.
[18] G. Orchard, E. P. Frady, D. B. D. Rubin, S. Sanborn, S. B. Shrestha, F. T. Sommer, M. Davies, in *2021 IEEE Workshop on Signal Processing Systems (SiPS)*, IEEE, Piscataway, NJ **2021**, pp. 254–259.
[19] C. Frenkel, J.-D. Legat, D. Bol, *IEEE Trans Biomed Circuits Syst* **2019**, *13*, 999.
[20] L. Alvado, J. Tomas, S. Saıghi, S. Renaud, T. Bal, A. Destexhe, G. Le Masson, *Neurocomputing* **2004**, *58*, 109.
[21] C. Adda, L. Cario, J. Tranchant, E. Janod, M.-P. Besland, M. Rozenberg, P. Stoliar, B. Corraze, *MRS Communications* **2018**, *8*, 835.
[22] P. Stoliar, J. Tranchant, B. Corraze, E. Janod, M.-P. Besland, F. Tesler, M. Rozenberg, L. Cario, *Adv. Funct. Mater.* **2017**, *27*, 1604740.
[23] G. T. Einevoll, A. Destexhe, M. Diesmann, S. Grün, V. Jirsa, M. de Kamps, M. Migliore, T. V. Ness, H. E. Plesser, F. Schürmann, *Neuron* **2019**, *102*, 735.
[24] M. Colombo, *J. Exp. Theor. Artif. Intell.* **2017**, *29*, 361.
[25] H. De Garis, C. Shuo, B. Goertzel, L. Ruiting, *Neurocomputing* **2010**, *74*, 3.
[26] T. Yamazaki, J. Igarashi, H. Yamaura, *Neuroscience* **2021**, *462*, 235.
[27] A. L. Hodgkin, A. F. Huxley, *J. Physiol.* **1952**, *117*, 500.
[28] M. Khodashenas, G. Baghdadi, F. Towhidkhah, *J Math. Neurosci.* **2019**, *9*, 1.
[29] Z. Zhu, Z. Deng, Q. Wang, Y. Wang, D. Zhang, R. Xu, L. Guo, H. Wen, *Front Pharmacol* **2022**, *13*, 939555.
[30] E. M. Izhikevich, *Dynamical systems in neuroscience*, MIT press, Cambridge **2007**.
[31] J. M. Bower, D. Beeman, M. Hucka, *MIT Press*, Cambridge**2003**.
[32] E. Yavuz, J. Turner, T. Nowotny, *Sci. Rep.* **2016**, *6*, 18854.
[33] J. K. Eshraghian, M. Ward, E. O. Neftci, X. Wang, G. Lenz, G. Dwivedi, M. Bennamoun, D. S. Jeong, W. D. Lu, Proceedings of the IEEE **2023**, *111*, 9, pp. 1016–1054.
[34] L. P. Landsmeer, M. C. Engelen, R. Miedema, C. Strydis, *Neurocomputing* **2024**, *598*, 127953.
[35] L. Chua, V. Sbitnev, H. Kim, *Int. J. Bifurc. Chaos* **2012**, *22*, 1230011.
[36] M. P. Sah, H. Kim, L. O. Chua, *IEEE Circuits Syst. Mag.* **2014**, *14*, 12.
[37] N. Schweighofer, K. Doya, M. Kawato, *J. Neurophysiol.* **1999**, *82*, 804.
[38] M. Giugliano, M. Negrello, D. Linaro, *Computational modelling of the brain: modelling approaches to cells, circuits and networks*, vol. *1359*, Springer Nature, Berlin **2022**.
[39] L. Chua, *Semicond. Sci. Technol.* **2014**, *29*, 104001.
[40] M. Sah, A. Ascoli, R. Tetzlaff, V. Rajamani, R. K. Budhathoki, *J. Low Pow. Electron. Appl.* **2024**, *14*, 31.
[41] Y. Xu, J. Ma, X. Zhan, L. Yang, Y. Jia, *Cogn. Neurodyn.* **2019**, *13*, 601.
[42] B. Mohammad, M. A. Jaoude, V. Kumar, D. M. Al Homouz, H. A. Nahla, M. Al-Qutayri, N. Christoforou, *Nanotechnol. Rev.* **2016**, *5*, 311.
[43] S. Kumar, X. Wang, J. P. Strachan, Y. Yang, W. D. Lu, *Nat. Rev. Mater.* **2022**, *7*, 575.
[44] M. D. Pickett, G. Medeiros-Ribeiro, R. S. Williams, *Nat. Mater.* **2013**, *12*, 114.
[45] W. Yi, K. K. Tsang, S. K. Lam, X. Bai, J. A. Crowell, E. A. Flores, *Nat. Commun.* **2018**, *9*, 1.
[46] Y. Yang, X. Zhang, P. Chen, L. Cheng, Y. Ding, C. Li, J. Yu, Q. Liu, *IEEE Electron Device Lett.* **2024**, *45*, 2225.
[47] X. Hu, C. Liu, *Nonlinear Dyn.* **2019**, *97*, 1721.
[48] F. Corinto, A. Ascoli, S. K. Sung-Mo, in *2013 IEEE International Symposium on Circuits and Systems (ISCAS)*, IEEE, Piscataway, NJ **2013**, pp. 417–420.
[49] F. Corinto, M. Gilli, A. Ascoli, R. Tetzlaff, in *2013 European Conference on Circuit Theory and Design (ECCTD)*, IEEE, Piscataway, NJ **2013**, pp. 1–4.
[50] Y. Liu, H. H.-C. Iu, Y. Qian, *IEEE Transactions on Circuits and Systems II: Express Briefs* **2021**, *68*, 2982.
[51] Q. Xu, Y. Wang, B. Chen, Z. Li, N. Wang, *Chaos Solitons Fractals* **2023**, *172*, 113627.
[52] Q. Xu, Y. Wang, H. Wu, M. Chen, B. Chen, *Chaos Solitons Fractals* **2024**, *179*, 114458.
[53] X. Li, J. Sun, Y. Sun, C. Wang, Q. Hong, S. Du, J. Zhang, *IEEE Trans. Circuits Syst. Regul. Pap.* **2024**, *71*, 2320.
[54] M. S. Feali, A. Ahmadi, *Neural Proc. Lett.* **2017**, *45*, 1.
[55] H.-M. Huang, R. Yang, Z.-H. Tan, H.-K. He, W. Zhou, J. Xiong, X. Guo, *Adv. Mater.* **2019**, *31*, 1803849.
[56] M. D. Pickett, R. S. Williams, *Nanotechnology* **2012**, *23*, 215202.
[57] G. A. Gibson, *Adv. Funct. Mater.* **2018**, *28*, 1704175.
[58] S. Pearson, H. S. G. Anson, *Proc. Phys. Soc. London* **1921**, *34*, 175.
[59] H. Crane, in *1961 IEEE International Solid-State Circuits Conference. Digest of Technical Papers*, vol *4*, IEEE, Piscataway, NJ **1961**, pp. 30–31.
[60] H. Lim, V. Kornijcuk, J. Y. Seok, S. K. Kim, I. Kim, C. S. Hwang, D. S. Jeong, *Sci. Rep.* **2015**, *5*, 1.
[61] M. Salverda, R. Hamming-Green, B. Noheda, *J. Phys. D Appl. Phys.* **2022**, *55*, 335305.
[62] A. Ascoli, A. S. Demirkol, I. Messaris, V. Ntinas, D. Prousalis, S. Slesazeck, T. Mikolajick, F. Corinto, M. Bonnin, M. Gilli, P. P. Civalleri, R. Tetzlaff, L. Chua, *Adv. Electron. Mater.* **2025**, 2400789.
[63] A. Nabil, T. N. Kumar, H. A. F. Almurib, *IEEE J. Emerg. Sel. Top. Circ. Syst.* **2022**, *12*, 762.
[64] M. M. Gasparinatou, N. Matzakos, P. Vlamos, in *Worldwide Congress on "Genetics, Geriatrics and Neurodegenerative Diseases Research"*, Springer, Berlin **2022**, pp. 69–79.
[65] C. Guo, Y. Xiao, M. Jian, J. Zhao, B. Sun, *Microelectron. J.* **2023**, *136*, 105774.

[66] J. Bian, Z. Liu, Y. Tao, Z. Wang, X. Zhao, Y. Lin, H. Xu, Y. Liu, *Int. J. Extreme Manuf.* **2023**, *6*, 012002.
[67] R. Wang, J.-Q. Yang, J.-Y. Mao, Z.-P. Wang, S. Wu, M. Zhou, T. Chen, Y. Zhou, S.-T. Han, *Adv. Intell. Syst.* **2020**, *2*, 2000055.
[68] C. Du, F. Cai, M. A. Zidan, W. Ma, S. H. Lee, W. D. Lu, *Nat Commun* **2017**, *8*, 2204.
[69] D. Ju, S. Kim, *Adv. Funct. Mater.* **2024**, *34*, 2409436.
[70] R. Chaurasiya, L.-C. Shih, K.-T. Chen, J.-S. Chen, *Mater. Today* **2023**, *68*, 35.
[71] D. Kuzum, S. Yu, H. P. Wong, *Nanotechnology* **2013**, *24*, 382001.
[72] Y. Lin, F. Meng, T. Zeng, Q. Zhang, Z. Wang, Y. Cheng, X. Zhao, L. Gu, H. Xu, Y. Liu, *Adv. Funct. Mater.* **2023**, 2302787.
[73] R. Yang, H.-M. Huang, Q.-H. Hong, X.-B. Yin, Z.-H. Tan, T. Shi, Y.-X. Zhou, X.-S. Miao, X.-P. Wang, S.-B. Mi, C.-L. Jia, X. Guo, *Adv. Funct. Mater.* **2018**, *28*, 1704,455.
[74] C. Du, W. Ma, T. Chang, P. Sheridan, W. D. Lu, *Adv. Funct. Mater.* **2015**, *25*, 4290.
[75] S. Kim, C. Du, P. Sheridan, W. Ma, S. Choi, W. D. Lu, *Nano Lett.* **2015**, *15*, 2203.
[76] Z. Q. Wang, H. Y. Xu, X. H. Li, H. Yu, Y. C. Liu, X. J. Zhu, *Adv. Funct. Mater.* **2012**, *22*, 2759.
[77] A. Khanas, C. Hebert, L. Becerra, X. Portier, N. Jedrecy, *Adv. Electron. Mater.* **2022**, *8*, 2200421.
[78] I. Margolin, A. Chouprik, V. Mikheev, S. Zarubin, D. Negrov, *Appl. Phys. Lett.* **2022**, *121*, 10.
[79] V. Mikheev, A. Chouprik, Y. Lebedinskii, S. Zarubin, Y. Matveyev, E. Kondratyuk, M. G. Kozodaev, A. M. Markeev, A. Zenkevich, D. Negrov, *ACS Appl. Mater. Interfaces* **2019**, *11*, 32108.
[80] G. C. Adam, A. Khiat, T. Prodromakis, *Nat Commun* **2018**, *9*, 5267.
[81] N. C. Dao, D. Koch, in *2020 International Conference on Electronics, Information, and Communication (ICEIC)*, IEEE, Piscataway, NJ **2020**, pp. 1–6.
[82] X.-D. Li, N.-K. Chen, B.-Q. Wang, M. Niu, M. Xu, X. Miao, X.-B. Li, *Adv. Mater.* **2024**, *36*, 2307951.
[83] Y. Li, Z. Wang, R. Midya, Q. Xia, J. J. Yang, *J. Phys. D Appl. Phys.* **2018**, *51*, 503002.
[84] J. A. White, J. T. Rubinstein, A. R. Kay, *Trends Neurosci.* **2000**, *23*, 131.
[85] A. A. Faisal, in *Computational Systems Neurobiology*, Springer, Berlin **2012**, pp. 227–257.

Lennart P. L. Landsmeer received the M.Sc. degree in Nanobiology at Delft University of Technology in 2023 and worked shortly as a scientific coworker at Forschungszentrum Jülich, Germany. He is currently pursuing a Ph.D. degree at the Quantum and Computer Engineering Department of Delft University of Technology, working on a joint project with the Neuroscience Department of the Erasmus Medical Center, The Netherlands.

Muhammad Ali Siddiqi is an Assistant Professor of Electrical Engineering at the Lahore University of Management Sciences (LUMS), Pakistan. He holds a Ph.D. from Erasmus University Medical Center, Rotterdam, where he researched the security and privacy of Implantable Medical Devices. He previously worked as a postdoctoral researcher at TU Delft on in-memory computing for lightweight cryptography and neural implants, and as a Design Engineer at Silicon Labs Norway. He is a Technical Program Committee member of the Reconfigurable Architectures Workshop (RAW). His research interests include low-power hardware design, brain-machine interfaces, and the cybersecurity of implantable and wearable devices.

Heba Abunahla is an Assistant Professor in the Department of Quantum and Computer Engineering at TU Delft. Her research covers resistive random-access memory (ReRAM), neuromorphic computing, 2D materials-based electronics, biosensing, and hardware security. She is actively involved in international collaborations and has published widely in the field of emerging computing technologies. Dr. Abunahla also serves as a Review Editor for Frontiers in Neuroscience, focusing on brain-inspired computing. She is a core member of the EEMCS Diversity and Inclusion Team at TU Delft and was awarded the Unique Fellowship for Top Female Academic Scientists in 2022.

Mario Negrello is an assistant professor of neuroscience at Erasmus Medical Center in Rotterdam, combining empirical and computational research. He holds a mechanical engineering degree, a masters and a PhD in Cognitive Science (summa cum laude) from the University of Osnabrück. His research career path included research on embodied neural networks Fraunhofer Institute, a visiting position at Cornell, postdoctoral work on cerebellar modeling at the Okinawa Institute of Science and Technology. He has published widely in neuroscience, robotics, and machine learning, co-edited the book Computational Modelling of the Brain (Springer, 2023), and authored the monograph Invariants of Behavior (Springer, 2012).

Said Hamdioui is Chair Professor at TU Delft and Head of the Computer Engineering Lab. His research spans emerging computing technologies (e.g., in-memory and brain-inspired computing) and hardware dependability (e.g., test, reliability). He has over 330 publications, four patents, and extensive industry experience at Intel, Philips, and NXP. A leader in global research, he serves on editorial boards and has earned over 20 Best Paper Awards and multiple innovation honors. Hamdioui is an IEEE Senior Member, Netherlands Academy of Engineering Fellow, and part of Stanford's World's Top 2% Scientists list.

Christos Strydis is an associate professor jointly appointed at Erasmus MC's Neuroscience department and TU Delft's Quantum & Computer Engineering department. He leads the Neurocomputing Laboratory and is a senior IEEE member. He earned his BSc in Electronics & Computer Engineering (magna cum laude) from the Technical University of Crete and his MSc and PhD from TU Delft. His research spans biologically plausible brain simulations, next-generation neural implants, and ultrasound-based brain imaging. He has been awarded multiple national and EU projects, served on international program committees, published widely, and supervised numerous students across all academic levels.